Impact of individual acute phase serum amyloid A isoforms on HDL metabolism in mice[s]

Myung-Hee Kim,* Maria C. de Beer,[†,§] Joanne M. Wroblewski,[*,§] Richard J. Charnigo,**
Ailing Ji,[*,§] Nancy R. Webb,[§,††] Frederick C. de Beer,[*,§] and Deneys R. van der Westhuyzen[1,*,§,§§]

Departments of Internal Medicine,* Physiology,[†] Pharmacology and Nutritional Sciences,[††] and Molecular and Cellular Biochemistry,[§§] and Saha Cardiovascular Research Center,[§] University of Kentucky Medical Center, Lexington, KY 40536; and Departments of Statistics and Biostatistics,** University of Kentucky, Lexington, KY 40506

Abstract   The acute phase (AP) reactant serum amyloid A (SAA), an HDL apolipoprotein, exhibits pro-inflammatory activities, but its physiological function(s) are poorly understood. Functional differences between SAA1.1 and SAA2.1, the two major SAA isoforms, are unclear. Mice deficient in either isoform were used to investigate plasma isoform effects on HDL structure, composition, and apolipoprotein catabolism. Lack of either isoform did not affect the size of HDL, normally enlarged in the AP, and did not significantly change HDL composition. Plasma clearance rates of HDL apolipoproteins were determined using native HDL particles. The fractional clearance rates (FCRs) of apoA-I, apoA-II, and SAA were distinct, indicating that HDL is not cleared as intact particles. The FCRs of SAA1.1 and SAA2.1 in AP mice were similar, suggesting that the selective deposition of SAA1.1 in amyloid plaques is not associated with a difference in the rates of plasma clearance of the isoforms. Although the clearance rate of SAA was reduced in the absence of the HDL receptor, scavenger receptor class B type I (SR-BI), it remained significantly faster compared with that of apoA-I and apoA-II, indicating a relatively minor role of SR-BI in SAA's rapid clearance.[Jlr] These studies enhance our understanding of SAA metabolism and SAA's effects on AP-HDL composition and catabolism.—Kim, M-H., M. C. de Beer, J. M. Wroblewski, R. J. Charnigo, A. Ji, N. R. Webb, F. C. de Beer, and D. R. van der Westhuyzen. Impact of individual acute phase serum amyloid A isoforms on HDL metabolism in mice. *J. Lipid Res.* 2016. 57: 969–979.

The acute phase (AP) response is a primary systemic inflammatory response to injury and infection. It can lead to a dramatic increase in the level of AP proteins in the circulation and, ultimately, contribute to the resolution of the inflammatory response and healing process. Serum amyloid A (SAA) is one of the most striking AP reactants that can rapidly increase up to a 1,000-fold or more in plasma concentration with appropriate stimuli (1, 2). SAA is found in AP plasma mainly as an apolipoprotein of HDL (3) and is produced largely by the liver in response to pro-inflammatory cytokines, including IL-1β, IL-6, and TNFα, which are released from macrophages exposed to inflammatory agents (4, 5). Following removal of inflammatory stimulants, SAA is cleared rapidly over ∼72 h, suggesting that SAA clearance/catabolism may be important to the homeostasis of inflammatory events (1).

In chronic inflammatory diseases, such as rheumatoid arthritis, atherosclerosis, Crohn's disease, obesity, and diabetes, plasma concentrations of SAA are also elevated and are maintained at more moderate concentrations. SAA levels have been linked to atherosclerotic cardiovascular disease (6). However, the physiological functions of SAA during chronic or AP inflammation are poorly understood. Human SAA has been implicated in several potentially important functions, such as monocyte chemotaxis, endothelial dysfunction, cytokine induction, subendothelial lipoprotein retention, and induction of matrix metalloproteinases (7–11). However, these reports were largely based on data obtained using a commercially available recombinant human SAA, a molecule that differs significantly from naturally occurring SAA in containing an N-terminal methionine and amino acid sequences of both human SAA1 and SAA2. Recently, it has been suggested that this recombinant SAA exerts effects not shown by native SAA

Abbreviations: AP, acute phase; CE, cholesterol ester; CETP, cholesteryl ester transfer protein; CETPtg, cholesteryl ester transfer protein transgenic; FC, free cholesterol; FCR, fractional clearance rate; Kfast, fast phase rate constant; LPS, lipopolysaccharide; N-HDL, normal HDL; PL, phospholipid; SAA, serum amyloid A; SAAKO mice, mice lacking SAA1.1/SAA2.1; SAA1.1KO mice, mice lacking SAA1.1; SAA2.1KO mice, mice lacking SAA2.1; SR-BI, scavenger receptor class B type I; TC, total cholesterol.

[1] To whom correspondence should be addressed.
  e-mail: dvwest1@uky.edu

[s] The online version of this article (available at http://www.jlr.org) contains a supplement.

(12, 13). Native SAA has been shown to alter both the protein and lipid composition of AP-HDL (14) and also to influence HDL remodeling (15) and cholesterol efflux from cells (16). Although several studies have reported that inflammation impedes reverse cholesterol transport to the liver (17–19), we have recently shown that impairment of reverse cholesterol transport in mice during inflammation does not depend on SAA (20). An absence of SAA also did not affect atherosclerosis in an apoE-deficient mouse model (21). However, SAA was shown to enhance abdominal aortic aneurysm in an angII-dependent abdominal aortic aneurysm mouse model (22).

The SAA gene family is highly conserved in mammals, comprising four closely related genes. Human *SAA1* and *SAA2* encode for the two major AP proteins, SAA1 and SAA2 (designated SAA1.1 and SAA2.1, respectively, in mice). The *SAA1* and *SAA2* genes are present in a gene cluster on human chromosome 11p15.1 and are coordinately induced during inflammation (23). *SAA3* is a pseudo-gene in humans (24), but is expressed in mice. *SAA4* is constitutively expressed and is present at low levels in both normal and AP plasma (1). Mouse SAA1.1 and SAA2.1 share 91% amino acid sequence identity and, like their human homologs, are highly induced during inflammation.

SAA has been shown to be a precursor of amyloid A protein, the main component of reactive systemic amyloid that may be deposited in organs as a result of chronic inflammation (25, 26). Reactive systemic amyloid A amyloidosis can complicate chronic inflammatory disorders that are associated with a sustained AP response. Interestingly, although murine SAA1.1 and SAA2.1 are produced at similar rates in the liver in response to cytokines, only SAA1.1 is deposited into amyloid fibrils in mice (27). Similarly, SAA1 is the predominant isoform deposited in amyloid fibrils in humans (28). With regard to other possible functional differences between the two isoforms, murine SAA2.1, but not SAA1.1, has been reported to suppress ACAT and to stimulate cholesterol ester hydrolase (CEH), functions that both might promote cholesterol efflux (29). Together, these findings demonstrate that SAA isoforms can have different metabolic functions and fates.

Several studies have investigated SAA catabolism in mice (30, 31) and in monkeys (32, 33). Because SAA1.1 and SAA2.1 are present in the same lipoprotein fraction in plasma and have a similar molecular mass, as well as amino acid sequence, it has been difficult to determine plasma degradation rates of these individual isoforms in naturally occurring HDL. In this study, we have used mice deficient in either SAA1.1 or SAA2.1 to investigate SAA isoform clearance rates and the effects of these SAA isoforms on HDL structure and composition, as well as their effects on HDL apolipoprotein clearance.

MATERIALS AND METHODS

Generation of SAA1.1KO and SAA2.1KO mice

Targeted deletion of the *SAA1.1* gene and the *SAA2.1* gene was performed by InGenious Targeting Laboratory, Inc. (Stony Brook, NY). The two genes are located approximately 9 kb apart, but in opposite orientation, on chromosome 7. For the SAA1.1KO mouse, a 15.9 kb region was used to construct the targeting vector. The region was designed such that the short homology arm extended ∼2.1 kb and the long homology arm ∼8.5 kb, 5′ and 3′ respectively, of a loxP/FRT floxed neo cassette. This cassette replaced ∼5.3 kb of the *SAA1.1* gene including exons 2-4 and the translation start codon. For the SAA2.1KO mouse, a 12.5 kb region was used to construct the targeting vector. The short homology arm extended ∼2.0 kb and the long homology arm ∼8.1 kb, 3′ and 5′ respectively, of a neo cassette that replaced 2.4 kb of the *SAA2.1* gene including exons 2-4 and the start codon. Cholesteryl ester transfer protein (CETP) transgenic (CETPtg) mice (B6.CBA-Tg(CETP)5203Tall/J) were obtained from the Jackson Laboratory. CETPtg mice were crossed with scavenger receptor class B type I (SR-BI)KO mice (generously provided by Dr. M. F. Linton) to generate CETPtg/SR-BIKO mice. All mice were on a C57BL/6 background and 8–12 weeks of age.

Mice were maintained in a pathogen-free facility under equal light-dark cycles with free access to water and food. An AP response was elicited by intraperitoneal injection of lipopolysaccharide (LPS) (*Escherichia coli* 0111:B4; Sigma Chemical Co.) at a dose indicated for the individual experiments. Plasma and HDL lipids were measured with enzymatic kits (Wako Chemicals). All procedures were carried out in accordance with United States Public Health Service policy and approved by the Veterans Affairs Medical Center Institutional Animal Care and Use Committee (Assurance number A3506-01).

HDL isolation, characterization, and radiolabeling

Plasma from 15–25 mice (equal numbers of male and female mice) was pooled for HDL isolation by sequential density gradient ultracentrifugation (d = 1.063–1.21 g/ml) (3). For the preparation of HDL from AP mice, mice were injected with LPS (6 µg/g) 24 h before plasma collection. HDL was dialyzed against 150 mM NaCl and 0.01% EDTA, sterile filtered, and stored under argon gas at 4°C. HDL protein concentrations were determined by the method of Lowry et al. (34). HDL was characterized by SDS-PAGE (4–20% polyacrylamide SDS gels) and gradient gel electrophoresis (4–20% nondenaturing polyacrylamide gels on which HDL was electrophoresed for 3.5 h at 200 V, 4°C). HDL apolipoproteins were radiolabeled with ^{125}I following the method of Bilheimer, Eisenberg, and Levy (35). HDL lipids were measured with enzymatic kits (439-17501, cholesterol; 461-08992 and 461-09092, TGs; 435-35801, free cholesterol (FC); and 433-36201, phospholipids (PLs); Wako Chemicals) and average values of three different HDL preparations are reported.

Electrofocusing

Aliquots (7 µl) of plasma from mice injected with LPS (4 µg/g) were subjected to electrofocusing as described, using an Ampholine gradient consisting of 20% (v/v) ampholines (pH 3–10), 40% (v/v) ampholines (pH 4–6.5), and 40% (v/v) ampholines (pH 7–9) (Pharmacia LKB Biotechnology, Inc.). Electrofocused samples were subjected to immunochemical analysis of SAA, as previously described (36).

Lipoprotein cholesterol distributions

Lipoprotein classes were separated by gel filtration chromatography and their cholesterol content determined as described previously (37). Briefly, plasma aliquots were diluted to 0.5 µg total cholesterol (TC) per microliter with 0.9% NaCl and 0.05% EDTA/NaN₃, and centrifuged to remove any particulate debris. Aliquots (40 µl) of the diluted samples were injected into a Superose 6 10/300 (GE Healthcare Life Sciences) chromatography

column by means of an autosampler set at 4°C (Agilent Technologies; G1329A) and the lipoprotein classes separated at a flow rate of 0.4 ml/min. The effluent was mixed with TC enzymatic reagent (Pointe Scientific) to allow for cholesterol determination. The absorbance of the reaction mixture at 500 nm was integrated using Agilent OpenLAB Software Suite (Agilent Technologies) and normalized to the TC concentration of the sample.

Real-time PCR

Total RNA was isolated from mouse liver using TRIzol reagent (Invitrogen) according to manufacturer's protocol. RNA samples were treated with TURBO DNA-free (Ambion) two times for 30 min at 37°C. RNA (1 μg) was reverse transcribed into cDNA using a high capacity cDNA reverse transcription kit (Applied Biosystems). After 4-fold dilution, 5 μl was used as a template for quantitative real-time PCR. Amplification was done for 40 cycles using Power SYBR Green PCR Master Mix kit (Applied Biosystems). Quantification was performed in duplicate using the standard curve method and normalized to 18S. The primers used for various genes are shown in supplementary Table 1.

Cellular cholesterol efflux determination

Cellular cholesterol efflux experiments in ABCG1-inducible BHK cells were carried out essentially as described (38). Cells (∼70% confluent) in 12-well plates were labeled with 0.2 μCi/ml [³H]cholesterol (35–50 Ci/mmol; Amersham Biosciences) in complete DMEM medium for 48 h. Cells were then washed three times with PBS containing 1 mg/ml BSA (PBS-BSA) and equilibrated overnight in DMEM containing 0.2% fatty acid-free BSA (DMEM-BSA) during which time ABCG1 expression was induced with 10 nM mifepristone. Control cells received no mifepristone. Following two additional washes with PBS-BSA, cells were incubated for 5 h at 37°C in DMEM-BSA with or without WT HDL, SAA1.1KO HDL, SAA2.1KO HDL, or SAAKO HDL, as indicated. Following incubation, the medium was collected and centrifuged to remove detached cells. Adherent cells were washed twice with PBS-BSA at 4°C and twice with PBS. Radioactivity in the media was measured in a Packard β liquid scintillation counter. Cellular lipid was extracted with hexane/isopropyl alcohol (3:2 v/v) for 30 min at room temperature and counted for radioactivity. Efflux of cellular [³H]cholesterol to media was expressed as the percentage of total radioactivity in media and cells. ABCG1-specific values were calculated as the difference between the efflux values in mifepristone-treated and control cells.

HDL clearance and apolipoprotein turnover studies

HDL clearance studies were performed essentially as described (14) by injecting normal or AP mice (1 μg/g LPS) with ¹²⁵I-labeled autologous or nonautologous HDL, as set out in figure legends. Mice were injected via the tail vein with 10 μg ¹²⁵I-HDL diluted in 100 μl saline. Recipient mice were fasted throughout the study, but had free access to water. Blood samples (∼50 μl aliquots) were obtained via retro-orbital bleeds at the indicated times, and plasma samples, now containing the radiolabeled HDL, were counted in a γ counter (Packard Cobra II auto γ). Plasma decay curves were generated by expressing the radioactivity at each time point as a percentage of the radioactivity determined 3 min after tracer injection. In experiments to determine the clearance rates of individual apolipoproteins, aliquots of plasma containing equal radioactivity at the different time points were first subjected to SDS-PAGE and the stained and dried gels were then subjected to autoradiography to identify the specific apolipoprotein bands. Apolipoprotein bands of interest were then excised and counted in a γ counter. Values of each sample were determined by correcting the radioactivity associated with each excised

band for volume of plasma loaded on the gel. Clearance rate determinations were performed for each of the five animals per group.

Analysis of plasma apolipoprotein clearance curves was performed using GraphPad PRISM software, which was used to fit the two-phase exponential clearance curves for each mouse. Plateau values were constrained to zero. The biphasic fit generated rate constants for the fast and slow pools and their relative pool sizes, which were used to calculate weighted average fractional clearance rates (FCRs) for the different apolipoproteins in the plasma for each mouse (39). Mean FCR values for each experimental group were calculated from the individual FCR values determined in five mice.

Statistical analysis

Data are presented as mean ± SE. Statistical comparisons for Table 1, Fig. 2, and supplementary Fig. 2 were based on one- or two-way ANOVA with observations weighted based on group variances. Statistical comparisons for Table 2 and related figures were based on unpaired t-tests (or one-way ANOVA) and paired t-tests. Benjamini-Hochberg multiplicity adjustments were pursued as appropriate for post hoc tests. Version 9.3 of SAS (SAS Institute, Cary, NC) was used for statistical comparisons. P values less than 0.05 are considered statistically significant and denoted in tables or figures with a single asterisk; P values less than 0.01 and 0.001 are denoted with two and three asterisks, respectively.

RESULTS

Expression of SAA isoforms in isoform-specific KO mice

The two major murine AP SAAs, SAA1.1 and SAA2.1, have almost identical sequences and the proteins share 91% amino acid identity. SAA1.1KO and SAA2.1KO mice were generated as described in the Materials and Methods and in supplementary Fig. 1A, B. The deletion of the individual SAA isoforms was confirmed by isoelectric focusing of plasma from LPS-injected isoform-specific mice lacking either SAA1.1 or SAA2.1 (**Fig. 1**), and was consistent with the lower levels of total SAA mRNA detected in the two isoform-specific KO mice compared with WT mice (supplementary Fig. 2). SAA was undetectable in plasma from nonacute control mice (data not shown). Both SAA isoforms are highly induced by LPS and the relative levels of protein and mRNA suggest that induction may be lower for SAA1.1 than for SAA2.1.
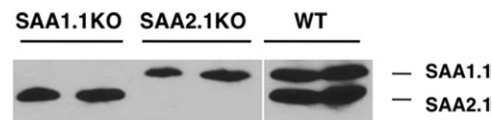

Fig. 1. Plasma SAA isoforms. Plasma was collected from WT, SAA1.1KO, and SAA2.1KO mice 24 h after administration of LPS (4 μg/g). The figure is from a representative experiment in which plasma aliquots (7 μl) were subjected to electrofocusing as set out in the Materials and Methods followed by blotting for SAA (rabbit anti-mouse SAA antisera, De Beer laboratory). Each lane represents plasma from a single mouse.

Impact of SAA1.1 or SAA2.1 on plasma lipid levels

The impact of an AP response on the plasma lipid levels of WT, SAA1.1KO, and SAA2.1KO mice is shown in **Fig. 2**. A robust AP response was elicited by administering LPS (4 μg/g body weight), whereas control mice received saline. The plasma lipid levels of WT mice treated similarly are shown for comparison. Consistent with our previously published report on SAAKO mice (14), plasma TC was modestly, but significantly, increased in female WT, SAA1.1KO, and SAA2.1KO mice after LPS injection. In contrast, in male WT, SAA1.1KO, and SAA2.1KO mice, plasma TC values were decreased significantly by LPS administration and did not exhibit the elevated TC previously observed in LPS-injected SAAKO mice (14); with respect to the different groups, no effect of genotype on TC was observed and no interaction between genotype and LPS effect was evident. In contrast to plasma TC, HDL cholesterol was reduced following LPS administration in both female ($P < 0.01$) and male ($P < 0.001$) WT and single KO mice, in agreement with data published for other mammals (40–43). There were no effects of genotype on HDL cholesterol and no interaction between genotype and LPS effect.

Previous reports (44, 45) have indicated elevated plasma TG levels in mice during the AP. We observed increased TG levels during the AP in male WT, SAA1.1KO, and SAA2.1KO mice ($P < 0.001$), but not in female mice. There were no effects of genotype on TG levels and no interactions

between genotype and LPS effect. We previously published that an LPS-induced AP response significantly increased plasma PL levels in SAAKO mice (14). This was not observed in mice lacking only one SAA isoform, and plasma PL was actually reduced in male LPS-injected SAA2.1KO mice ($P < 0.001$). In summary, plasma lipids were relatively similar in WT, SAA1.1KO, and SAA2.1KO mice under normal conditions. In response to LPS, plasma lipids underwent significant changes, most prominently, decreases in HDL cholesterol in all three genotypes and significant increases in plasma TGs in male mice only.

The impact of SAA isoforms on plasma lipoprotein distribution

The potential impact of the SAA isoforms on plasma lipoprotein profiles in the AP was analyzed by fast protein liquid chromatography. As shown in Supplementary Fig. 3A, B, in both male and female mice, overall lipoprotein cholesterol profiles of the three different genotypes were similar with respect to both the size of the different lipoprotein fractions (VLDL, LDL, and HDL) as well as their cholesterol levels.

Characterization of AP-HDL from SAA1.1KO and SAA2.1KO mice

HDL (density, 1.063–1.21 g/ml) was isolated by sequential ultracentrifugation from the plasma of SAA1.1KO, SAA2.1KO, and control WT mice, obtained 24 h after the
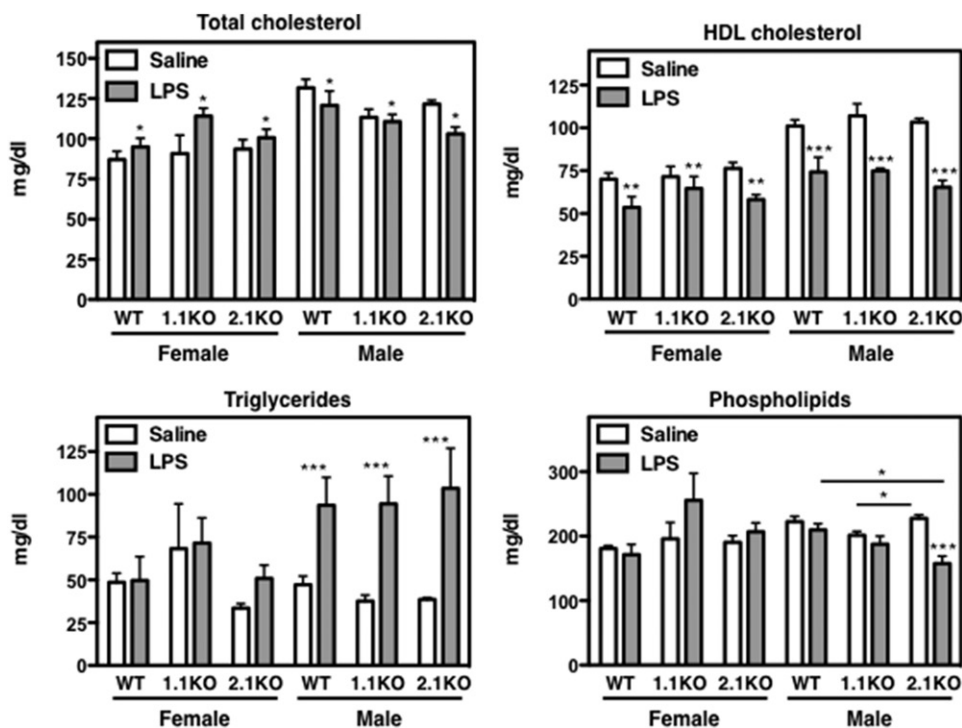

Fig. 2. Plasma lipids of WT, SAA1.1KO, and SAA2.1KO mice. Plasma was collected from individual male and female WT, SAA1.1KO, and SAA2.1KO mice 24 h after intraperitoneal administration of saline or 4 μg/g LPS for the determination of plasma lipid concentrations. TC, HDL cholesterol, PLs, and TGs were determined enzymatically with commercial kits (Wako Chemicals). Values represent the mean ± SEM. *$P < 0.05$, **$P < 0.01$, ***$P < 0.001$ saline versus LPS for each group. In male mice significant differences in plasma PL between genotypes are also indicated; *$P < 0.05$; n = 5.

injection of saline [normal HDL (N-HDL)] or 6 µg/g LPS (AP-HDL). HDL apolipoprotein composition was analyzed in a Coomassie-stained SDS gel and showed the expected presence of SAA only in AP-HDLs (**Fig. 3A**). AP-HDL from WT mice was shown on a separate gel for comparison to the HDLs from SAA1.1KO and SAA2.1KO mice. SAA was present at similar levels in each of the AP-HDLs from single KO mice, where it was the second most abundant HDL apolipoprotein. The normal low level of apoE was also increased in the AP-HDLs from both single KO mice, as was also reported for AP-HDL from WT and SAAKO mice (14). As previously shown, AP-HDL from WT mice migrated on nondenaturing gradient gel electrophoresis as larger-sized particles compared with N-HDL (14) (Fig. 3B). The AP-HDLs from LPS-injected SAA1.1KO and SAA2.1KO mice migrated similarly to the AP-HDL from WT mice with an apparent increased Stokes radius, and no size difference was evident between the two SAAKO genotypes. We have shown that AP-HDL from SAAKO mice also migrates similarly to WT AP-HDL (14). Thus, the absence of one or both SAA isoforms did not substantially affect the apparent size of AP-HDL.

The protein/lipid composition of the different AP-HDLs is shown in **Table 1**. No significant differences between genotypes were observed regarding total protein, TG, and PL composition, either in LPS-treated or LPS-untreated mice. The AP-HDLs showed higher PL content for all genotypes, but this difference did not reach significance. These findings differ from our earlier finding that in response to

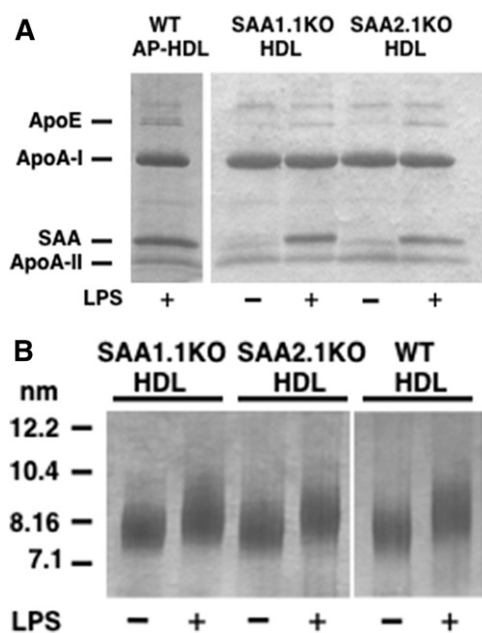**Fig. 3.** Characterization of HDL. HDL (d = 1.063–1.21) was isolated by sequential ultracentrifugation from pooled plasma from 15–20 WT, SAA1.1KO, and SAA2.1KO mice 24 h after the intraperitoneal injection of saline or LPS (6 µg/g). A: HDL apolipoproteins were separated by SDS-PAGE on a 4–20% acrylamide gel. B: HDL size was determined by nondenaturing gel electrophoresis using a 4–20% acrylamide gel. Protein loading was 5 µg HDL per lane and visualization was by Coomassie staining. Gels shown are representative of three separate lipoprotein preparations.

LPS, SAAKO HDL shows a significant decrease in protein and increase in PL content compared with WT HDL (14). This change occurred only in SAAKO HDL and not in WT HDL. With respect to cholesterol content, the AP response significantly increased the FC content of HDL ($P < 0.001$) and decreased the cholesterol ester (CE) content ($P < 0.001$) in each genotype, as previously shown in SAAKO mice (14). However, no significant genotype effect in determining FC and CE contents was evident. FC/CE ratios in AP-HDLs also showed no significant differences between genotypes, suggesting ACAT activity and cholesterol esterification of HDL cholesterol were unaltered.

Impact of SAA isoforms on HDL function in cellular cholesterol efflux

ABCG1 is known to utilize HDL as its preferred acceptor (46). Using the ABCG1-inducible BHK in vitro model system (46, 47), we previously showed that AP-HDL can enhance cellular cholesterol efflux mediated by ABCG1 and that it was likely the PL enrichment of AP-HDL and not the presence of SAA that was responsible for the altered efflux. In the present study, we utilized the same in vitro system to compare the influence of SAA1.1 and SAA2.1 on ABCG1-mediated efflux to AP-HDLs prepared from WT, SAA1.1KO, SAA2.1KO, and SAAKO mice. As shown in **Fig. 4**, each of the AP-HDLs mediated both ABCG1-dependent and -independent efflux. ABCG1-dependent efflux was approximately 40% higher for the SAA single and double KO AP-HDLs than for WT AP-HDL. However, no significant differences in efflux were seen between ABCG1-dependent efflux to SAA1.1KO AP-HDL and SAA2.1KO AP-HDL. There was also no significant difference in ABCG1-dependant efflux between SAAKO AP-HDL and either SAA1.1KO or SAA2.1KO AP-HDLs. Similar to ABCG1-dependent efflux, nonspecific efflux and total efflux values were, in all cases, significantly greater for the SAA-depleted AP-HDLs than for WT AP-HDL, although the differences between the WT AP-HDL and the SAA-depleted HDLs were not as great as for ABCG1-dependent efflux.

Plasma clearance of HDL apolipoproteins in normal and AP mice

To evaluate the rates of plasma clearance of individual HDL apolipoproteins in normal mice and AP mice, HDL was isolated from WT mice under normal healthy conditions (N-HDL) or mice in the AP 24 h following injection with LPS (AP-HDL). HDLs were radio-iodinated and the clearance of ^{125}I-N-HDL and ^{125}I-AP-HDL apolipoproteins were compared in control normal mice or AP mice. To specifically compare the clearance rates of individual apolipoproteins, plasma aliquots were collected at the indicated times after injection of ^{125}I-HDL and subjected to SDS-PAGE to separate the different apolipoproteins. Radioactivity in each band was determined and expressed as a percentage of the corresponding radioactivity detected at 3 min. Among the apolipoproteins of AP-HDL, SAA (FCR = 0.22 ± 0.03/h) was cleared at a significantly faster rate in AP mice than apoA-I (FCR = 0.062 ± 0.006/h) (**Fig. 5**;

	WT Saline (%)	WT LPS (%)	SAA1.1KO Saline (%)	SAA1.1KO LPS (%)	SAA2.1KO Saline (%)	SAA2.1KO LPS (%)
Protein	47.7 ± 1.40	44.9 ± 1.24	48.4 ± 1.71	48.1 ± 2.73	48.3 ± 1.89	46.5 ± 3.16
FC	4.1 ± 0.12	6.9 ± 0.59^a	3.7 ± 0.44	7.1 ± 0.69^a	4.1 ± 0.24	7.7 ± 0.51^a
CE	15.2 ± 0.36	12.3 ± 1.39^a	14.5 ± 1.12	9.0 ± 1.83^a	15.0 ± 0.74	9.7 ± 0.66^a
TGs	1.3 ± 0.52	1.5 ± 0.58	1.8 ± 0.65	1.5 ± 0.41	0.8 ± 0.09	1.1 ± 0.20
PLs	31.7 ± 1.33	34.4 ± 1.05	31.3 ± 2.72	34.3 ± 2.10	31.8 ± 2.07	34.9 ± 2.34

Values are the mean ± SEM of three HDL preparations for each group. CE was calculated as the difference between TC and FC.

[a] $P < 0.001$ for LPS-injected mice versus saline-injected mice.

Table 2, section A). apoA-II (FCR = 0.11 ± 0.01/h) cleared at an intermediate rate, which was significantly different from both apoA-I and SAA clearance rates. When AP-HDL clearance was analyzed in normal mice, SAA was again cleared more rapidly than apoA-I and apoA-II. Interestingly, whereas the clearance rate of apoA-I in AP-HDL was similar in normal and AP mice, the FCRs of both SAA and apoA-II in AP-HDL were more rapid in normal than in AP mice, although these differences did not reach significance. The rapid initial phase of clearance for both SAA and apoA-II from AP-HDL was also faster in normal mice than in AP mice. This was consistent with an observed increase in the fast phase rate constant (Kfast) for SAA in normal compared with AP mice (Kfast = 1.3 ± 0.24/h vs. 0.79 ± 0.14/h, respectively), although this difference did not reach significance.

The clearance rates of the apolipoproteins in N-HDL were also compared in normal and AP mice (Fig. 5; Table 2,

Fig. 4. ABCG1-mediated cholesterol efflux to AP WT HDL, SAA1.1KO HDL, SAA2.1KO HDL, and SAAKO HDL. Transfected BHK cells were labeled with [³H]cholesterol and then induced to express ABCG1 as described in the Materials and Methods. Cellular cholesterol efflux was measured during a 5 h incubation with 25 μg/ml AP WT HDL (white bars), AP SAA1.1KO HDL (light gray bars), AP SAA2.1KO HDL (dark gray bars), or AP SAAKO HDL (black bars). ABCG1-dependent efflux represents the difference between BHK cells treated with mifepristone (Total) and untreated cells (ABCG1-independent). The data shown are representative of three experiments each performed in triplicate. Values are the mean ± SEM. *$P < 0.05$, **$P < 0.01$, ***$P < 0.001$.

section A). The clearance rates of both apoA-I and apoA-II in N-HDL were similar to their respective clearance rates in AP-HDL. These results indicated that, in the AP, neither the presence of SAA nor other possible changes in AP-HDL exert a significant effect on the clearance of apoA-I or apoA-II, the two major apolipoproteins on N-HDL.

Plasma clearance of SAA isoforms

The SAA isoform-specific KO mice were used to investigate and compare the clearance rates of SAA1.1 and SAA 2.1 present in AP-HDL. AP-HDLs containing either SAA1.1 or SAA2.1 were prepared from AP SAA2.1KO and SAA1.1KO mice, respectively. Plasma clearance rates of the two SAA isoforms, as well as apoA-I and apoA-II, were then determined in syngeneic mice made AP by LPS injection. Thus SAA1.1KO mice received HDL prepared from SAA1.1KO mice (containing only the SAA2.1 isoform), and SAA2.1KO mice received HDL prepared from SAA2.1KO mice (containing only the SAA1.1 isoform). Clearance rates for the two SAA isoforms were not significantly different (FCR for SAA1.1 = 0.26 ± 0.02/h; SAA2.1 = 0.23 ± 0.03/h) (**Fig. 6**; Table 2, section B). The clearance rates of apoA-I and apoA-II were also not significantly different when compared in the two single KO strains. There was an apparent increase in the initial rate of clearance of SAA1.1 compared with SAA2.1, consistent with an increased fast phase rate constant (1.6-fold) compared with SAA2.1 clearance (Kfast SAA1.1 = 1.08 ± 0.07/h vs. SAA2.1 = 0.66 ± 0.07/h; $P = 0.0025$). Similar to SAA1.1, the fast phase rate constant of apoA-II was increased in the SAA2.1KO HDL compared with SAA1.1KO HDL (Kfast apoA-II = 0.98 ± 0.16 vs. apoA-II = 0.47 ± 0.06/h, respectively; $P = 0.02$). Together, these results show that the two AP SAA isoforms are cleared at similar rates from AP-HDL under AP conditions, although a difference in the initial fast clearance phase between the two SAA isoforms was observed.
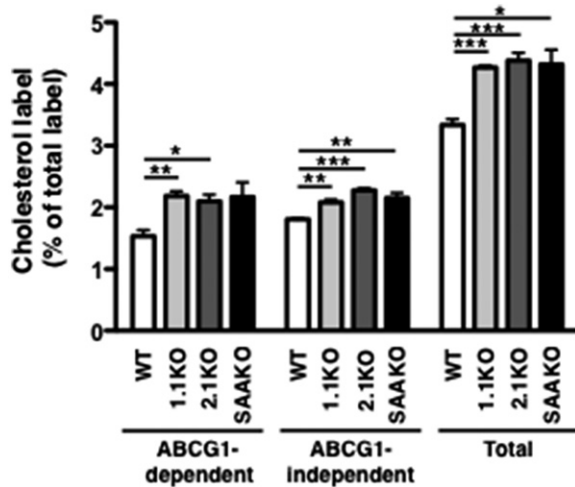
The role of SR-BI in clearance of HDL apolipoproteins

The scavenger receptor, SR-BI, plays a key role in the metabolism of HDL (48). SR-BI binds HDL through its high-affinity interaction with the apolipoproteins of HDL, including SAA (49), and mediates the selective lipid uptake of CEs into cells without requiring the endocytic uptake of intact HDL particles. In previous studies, we showed that SR-BI mediates cellular uptake of SAA from HDL at a much greater rate than apoA-I, suggesting that SR-BI may contribute to the plasma clearance of SAA (49).
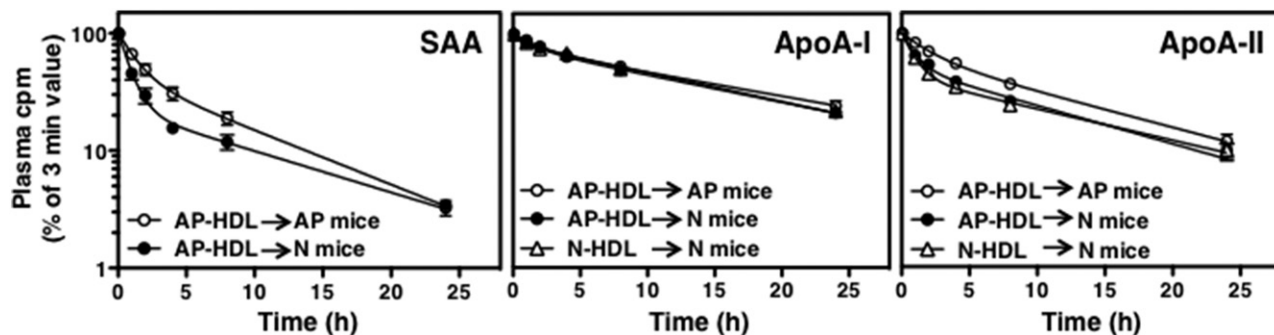
Fig. 5. Plasma clearance of apoA-I, apoA-II, and SAA from AP-HDL and N-HDL. ^{125}I-labeled AP-HDL or ^{125}I-N-HDL (30 μg) was intravenously administered to normal mice (N mice) or mice 24 h after injection of LPS (1 μg/g) (AP mice). Blood samples were collected at selected times up to 24 h after HDL administration and processed as set out in the Materials and Methods. Radioactivity at each time point is expressed as a percentage of the radioactivity at 3 min. Data were plotted with GraphPad Prism 4 as described in the Materials and Methods. The y axis represents radioactivity associated with apoA-I, apoA-II, and SAA proteins isolated by gel electrophoresis. Values plotted are mean ± SE, n = 5 mice.

To investigate the possible role of SR-BI in the rapid clearance of SAA, we studied the rate of SAA clearance in mice lacking SR-BI.

Because SRBI$^{-/-}$ mice have high levels of abnormally large HDL that has an altered lipid and apolipoprotein composition, clearance was examined in CETPtg mice and CETPtg mice crossed with SR-BI$^{-/-}$ mice. The expression of CETP in SRBI$^{-/-}$ mice results in the normalization of the size and plasma concentration of HDL (50), thereby providing a model for analyzing the role of SR-BI in the clearance of SAA from AP-HDL. For simplicity, the CETPtg mice are referred to as WT mice and CETPtg mice crossed with SR-BI$^{-/-}$ mice as SR-BIKO mice. The recipient mice in this experiment were not preinjected with LPS because we have previously shown SRBI$^{-/-}$ mice to be extremely sensitive to LPS (51). ^{125}I-AP-HDL was injected into WT mice or SR-BIKO mice. As shown in **Fig. 7** and Table 2, section C, the clearance rate of SAA in SR-BIKO mice was reduced (approximately 30%) compared with the clearance rate in WT mice (FCR = 0.39 ± 0.05/h and FCR = 0.57 ± 0.03/h, respectively; $P < 0.05$). In contrast, the clearance rates of apoA-I and apoA-II were not significantly altered by the absence of SR-BI in the SR-BIKO mice, consistent with previous findings that plasma levels of apoA-I were similar in WT and SR-BI$^{-/-}$ mice and the known function of SR-BI in mediating HDL-CE uptake selectively, without the uptake of HDL protein (52). These results indicate that although SR-BI may influence the clearance of SAA,

SAA's rapid clearance compared with apoA-I and apoA-II is not in large part dependent on SR-BI.

DISCUSSION

To better understand the metabolism of the AP SAA isoforms and their impact on HDL size, composition, and catabolism, we generated mice that lacked either SAA1.1 or SAA2.1. With respect to isoform gene expression, there was a lower abundance of SAA1.1 mRNA in the liver compared with SAA2.1 mRNA in the respective SAAKO mice, suggesting that while the two genes were coordinately regulated, either their rate of transcription or the stability of their two mRNAs differed. Plasma SAA levels were lower in both single KO mice compared with WT mice, indicating that, in the AP, the absence of one SAA isoform does not lead to a significant compensatory increase in the expression of the other isoform. Furthermore, the capacity of liver cells to transcribe, translate, and secrete one AP isoform is apparently not limited by the expression of the other isoform.

Infection and inflammation affect plasma lipids differently in different species. In humans and nonhuman primates, plasma TC typically declines during the AP (44, 53). In contrast, in rodents, plasma cholesterol increases during an AP response due to increased de novo cholesterol synthesis, reduced lipoprotein clearance, and a reduction

TABLE 2. FCRs

	Experiment	SAA FCR per Hour	ApoA-I FCR per Hour	ApoA-II FCR per Hour
A	AP-HDL → AP mice	0.22 ± 0.03	0.062 ± 0.006	0.11 ± 0.01
	AP-HDL → N mice	0.31 ± 0.03	0.072 ± 0.005	0.14 ± 0.01
	N-HDL → N mice	—	0.071 ± 0.004	0.14 ± 0.01
B	SAA1.1KO mice	(SAA2.1) 0.23 ± 0.03	0.093 ± 0.007	0.14 ± 0.01
	SAA2.1KO mice	(SAA1.1) 0.26 ± 0.02	0.077 ± 0.008	0.18 ± 0.01
C	AP-HDL → WT mice[a]	0.57 ± 0.03[b]	0.076 ± 0.003	0.12 ± 0.005
	AP-HDL → SR-BIKO mice[a]	0.39 ± 0.05	0.066 ± 0.002	0.14 ± 0.01

Values are the mean ± SE. For intra-experimental comparisons, differences between FCRs for SAA, apoA-I, and apoA-II were highly significant ($P < 0.01$). N mice, normal mice.

[a] Mice on a CETPtg background.

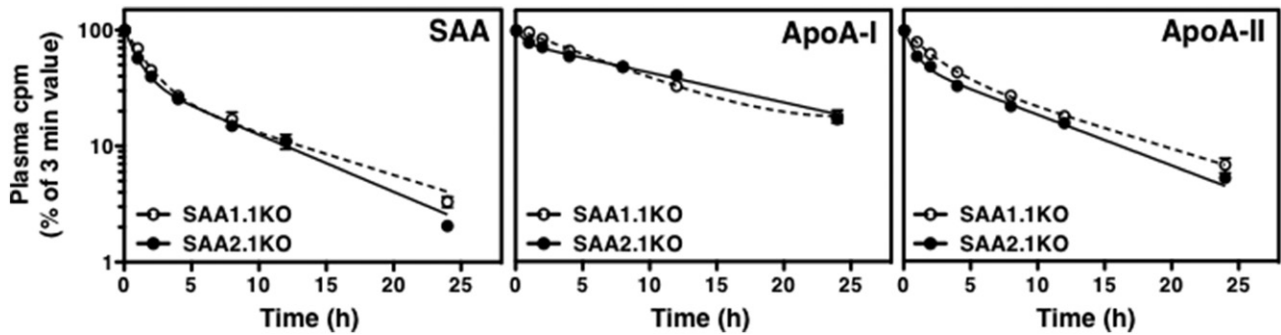[b] $P < 0.05$ for FCR of SAA in WT mice versus SR-BIKO mice.

Fig. 6. Plasma clearance of SAA1.1 and SAA2.1 from AP-HDL. ^{125}I-labeled AP-HDLs (30 μg) containing either SAA1.1 or SAA2.1, obtained from SAA2.1KO or SAA1.1KO mice, were intravenously administered to autologous mice 24 h after injection of LPS (1 μg/g). Blood samples were collected at selected times up to 24 h after HDL administration and processed as set out in the Materials and Methods. Radioactivity at each time point is expressed as a percentage of the radioactivity at 3 min. Data were plotted with GraphPad Prism 4 as described in the Materials and Methods. The y axis represents radioactivity associated with apoA-I, apoA-II, and SAA isoforms isolated by gel electrophoresis. Values plotted are mean ± SE, n = 5 mice.

in conversion of cholesterol to bile acids (44, 45). In the present study, although there was increased plasma cholesterol in WT, SAA1.1KO, and SAA2.1 female mice in the AP, there was actually a decrease in male mice, regardless of genotype. The observed gender effect is not understood. Like total plasma cholesterol, HDL cholesterol levels in the AP decline dramatically in humans (42) and nonhuman primates (44), as well as in rodents as reported in some (54), but not all (14, 44), studies. In this study, HDL cholesterol levels in both genders were similar in WT and the two single KO mice under normal conditions and were significantly reduced in the AP, although the reduction in the AP was more pronounced in male mice, which had higher HDL levels under normal conditions than female mice. Again, the observed effect of gender is unexplained.

The HDLs isolated from SAA1.1KO and SAA2.1KO mice exhibited expected changes in apolipoprotein composition. We reported previously that the presence of SAA

Fig. 7. Plasma clearance of SAA from AP-HDL in WT and SRBIKO mice. ^{125}I-labeled AP-HDL (30 μg) was intravenously administered to CETPtg (WT) and CETPtg mice lacking SR-BI (SRBIKO mice). Blood samples were collected at selected times up to 24 h after HDL administration and processed as set out in the Materials and Methods. Radioactivity at each time point is expressed as a percentage of the radioactivity at 3 min. Data were plotted with GraphPad Prism 4 as described in the Materials and Methods. Values are mean ± SE, n = 5 mice.

on AP-HDL from WT mice was offset by a reduction in apoA-I content, whereas apoA-II content did not vary significantly between normal and AP-HDLs (14). In the single SAAKO mice, the reduction in apoA-I content of AP-HDL to compensate for SAA was less evident, likely due to the fact that AP-HDLs from both single KO mice contained less SAA than AP-HDL from WT mice. Nondenaturing gel electrophoresis showed that SAA-containing AP-HDL from both SAA1.1KO and SAA2.1KO mice migrates as larger than normal particles, similar in size to AP-HDL from WT mice. The increased size of AP-HDL compared with N-HDL (3) has been attributed to the hydrophilic C-terminal end of SAA extending beyond the surface of the HDL particle (55). However, the fact that AP-HDLs from SAA-depleted mice also migrate as larger particles, indicates that changes other than SAA content are responsible for the increased size of AP-HDL (14).

Studies have indicated the two major SAA isoforms may have different metabolic fates and functions. In humans, the SAA1.1 isoform is preferentially deposited in amyloid fibrils (28), with some allelic variants being more amyloidogenic than others (56). Similarly, SAA1.1 is the predominant form in amyloid fibrils in mice (56). SAA isoforms have been reported to exhibit functional differences in their ability to affect cellular cholesterol efflux. SAA2.1, but not SAA1.1, was shown to both suppress ACAT in cells and to stimulate cholesterol esterase, effects that would be expected to promote cholesterol efflux (57). In the present study, we investigated whether the ability of HDL to promote efflux was differentially affected by SAA1.1 and SAA2.1. ABCG1-mediated cholesterol efflux was examined because HDL is the preferred cholesterol acceptor for this cholesterol transporter. Our results failed to show any significant difference between the two isoforms in their ability to promote or otherwise affect efflux. It remains possible that the isoforms may exert effects on efflux that are not detected in our assays. These might include effects that are independent of ABCG1 or elicited by lipid-poor SAA that is not associated with HDL, or by cell signaling events that are not elicited in our cell culture assay system.
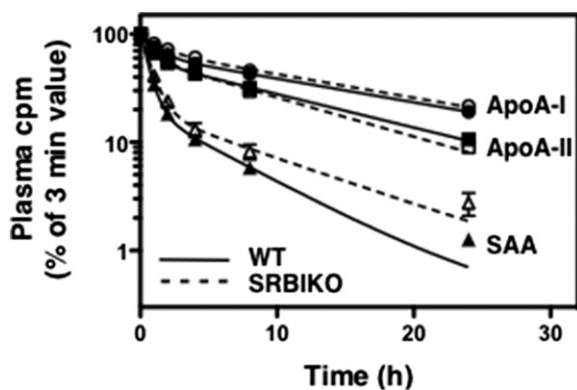
The current studies examined the plasma clearance rates of SAA and its two predominant isoforms, as well the effect of SAA on the plasma clearance of apoA-I and apoA-II. Results showed that SAA on HDL is cleared more rapidly from plasma than apoA-I, confirming previous findings carried out in mice (30, 58) and monkeys (32, 33). apoA-II was shown to have an intermediate FCR. The distinct FCRs of the three apolipoproteins support the notion that neither normal nor AP-HDL particles are cleared as intact particles, but rather through mechanisms that involve dissociation of apolipoproteins from HDL. The FCRs of apoA-I from normal and AP-HDLs were similar when measured in normal mice, suggesting that the presence of SAA on AP-HDL does not influence the clearance of apoA-I. This finding is consistent with the recent report that the displacement of an exchangeable fraction of apoA-I by SAA has only a minor effect on the structural stability of HDL particles (59). Similarly, the clearance rates of apoA-II in N-HDL and AP-HDL did not differ when measured in normal mice. When clearance of the AP-HDL was carried out in AP mice, clearance rates for both SAA and apoA-II, but not for apoA-I, were decreased compared with clearance rates in normal mice. The explanation for the selective negative impact of the AP on SAA and apoA-II plasma clearance is unclear. It is possible that AP-HDL has undergone remodeling in acute plasma that affects the turnover of some, but not all, apolipoproteins. Alternatively, the apolipoprotein clearance pathways in the normal and AP mice may differ.

To compare the turnover rates of SAA1.1 and SAA2.1, we isolated AP-HDL from SAA2.1KO and SAA1.1KO mice, respectively. This allowed us to study native AP-HDLs rather than HDLs that had undergone any type of reconstitution procedure necessitated by having to label specific apolipoproteins. FCRs were determined by injecting radiolabeled AP-HDL from SAA1.1KO or SAA2.1KO mice into syngeneic AP mice. Importantly, no significant difference was found between the FCRs of SAA1.1 and SAA2.1. We did, however, observe that SAA1.1 was cleared more rapidly by the fast phase component. A previous study, which examined mouse recombinant SAA isoforms that were reconstituted in normal or AP mouse HDL, also reported that SAA1.1 (previously termed SAA2) was more rapidly cleared than SAA2.1 (previously termed SAA1) in BALB/c mice, although only apparent half-life values and not FCR values were determined (31). However, the difference between the isoforms was only observed when clearance was measured either from reconstituted N-HDL or from AP-HDL analyzed in nonacute phase mice. Similarly, no significant difference was reported between the clearance rates of SAA1 and SAA2 in the AP in nonhuman primates (32). The similar rates of plasma clearance of the two SAA isoforms in AP mice suggest that the selective deposition of SAA1.1 in amyloid plaques (27) may not impact its rate of plasma clearance or reflect an increased clearance from HDL. In a previous study, Meek and Benditt (60) showed that plasma levels of SAA1.1 decline selectively compared with SAA2.1 in a casein-induced AP mouse model in which SAA1.1 is selectively deposited in

splenic tissue. Because the production and secretion of the two isoforms appeared to be similar in these mice, the data suggested that the selective loss of plasma SAA1.1 involved a selective and accelerated removal of the isoform from plasma, although plasma clearance rates were not directly measured. It is possible that the rate of SAA1.1 clearance is selectively altered under the conditions that lead to its selective deposition in casein-induced amyloid and that such conditions are not mimicked in the AP model used in the present study.

A possible role of SR-BI as a candidate receptor involved in SAA plasma clearance was examined. We (49) and others (61) showed that SR-BI is a high-affinity receptor for SAA that internalizes SAA at a markedly greater rate than apoA-I (49). Clearance was examined in control and SR-BI$^{-/-}$ mice that both overexpressed CETP. The plasma expression of CETP in SR-BI$^{-/-}$ mice normalizes the size and plasma concentration of HDL, thereby providing a model for analyzing the role of SR-BI in the clearance of SAA from AP-HDL (50). Our results show that the plasma clearance rates of apoA-I and apoA-II are not significantly altered in mice lacking SR-BI. In contrast, SAA clearance was significantly reduced (about 30%) in SR-BIKO mice. Although significant, this contribution of SR-BI to SAA clearance cannot account for the considerably faster plasma clearance rate (∼4-fold) of SAA compared with apoA-I. It is possible that SR-BI plays a role in mediating SAA uptake into cells, such as hepatocytes, but the rates of such uptake are evidently too low to markedly affect total plasma clearance rates.

The mechanisms responsible for the differential rates of removal of the different HDL apolipoproteins are poorly understood. In the case of apoA-I, clearance occurs mainly in the kidney and liver. Lipid-free/lipid-poor apoA-I particles are the preferred substrate for apoA-I uptake into the kidney (62), where it is filtered and then absorbed in kidney proximal tubules through the action of cubilin, a receptor for intrinsic factor-vitamin B12, with megalin serving as a coreceptor (63–65). A number of HDL-modifying processes can potentially generate small lipid-free/lipid-poor apoA-I particles. These include HDL remodeling within plasma, for example, through the actions or combined actions of CETP, hepatic and endothelial lipase, and SR-BI (15, 66, 67). Like apoA-I, apoA-II is also cleared through the kidney and can be reabsorbed through cubilin/megalin receptors. As shown in our study, apoA-II in mice is cleared more rapidly from plasma than apoA-I, but the reason(s) for this is unknown. Unfortunately, the biological identities of the slow and fast phases of clearance of apoA-II as well as SAA are not understood and the pathway(s) responsible for the relatively rapid plasma clearance of SAA remain undefined. Like apoA-II (68), SAA is more hydrophobic than apoA-I, binds strongly to HDL, and can displace apoA-I from HDL, at least in vitro (3, 69). The fact that the presence of SAA on AP-HDL does not alter the rate of apoA-I clearance suggests that SAA might not affect those processes that generate the lipid-free/lipid-poor apoA-I particles that serve as substrates for plasma apoA-I clearance.

Unlike the small, but important, fraction of apoA-I that exists in plasma as lipid-poor apoA-I or small lipid-poor preβ-HDL particles, SAA is found largely bound to lipoproteins, predominantly HDL. The mechanisms responsible for selective SAA dissociation or segregation from bulk HDL and the other major HDL apolipoproteins prior to SAA clearance are not understood. It should be noted that the present study examines the clearance rate of SAA that is present in mature HDL particles. It is possible that a fraction of SAA may be rapidly cleared from plasma before becoming part of mature HDL particles. Such a pathway would not be detected or quantified in our studies. The liver and kidney appear to be the major sites of SAA clearance in mice, although the rates of SAA tissue uptake have not been directly quantified (30). Aside from its uptake into liver, kidney, and other cell types, another process that might contribute to rapid plasma SAA clearance is the known ability of SAA to bind to cell-associated proteoglycans, including perlecan, located on epithelial cells in the circulatory system (70). It is possible that the initial rapid clearance phase of SAA is due, at least in part, to the binding of SAA to proteoglycans. The observation that SAA clears more slowly in AP mice than in normal mice may be the result of endogenous SAA saturating SAA proteoglycan binding sites.⬛

REFERENCES

1. Uhlar, C. M., and A. S. Whitehead. 1999. Serum amyloid A, the major vertebrate acute-phase reactant. *Eur. J. Biochem.* **265:** 501–523.

2. Kisilevsky, R., and S. P. Tam. 2002. Acute phase serum amyloid A, cholesterol metabolism, and cardiovascular disease. *Pediatr. Pathol. Mol. Med.* **21:** 291–305.

3. Coetzee, G. A., A. F. Strachan, D. R. van der Westhuyzen, H. C. Hoppe, M. S. Jeenah, and F. C. de Beer. 1986. Serum amyloid A-containing human high density lipoprotein 3. Density, size, and apolipoprotein composition. *J. Biol. Chem.* **261:** 9644–9651.

4. Selinger, M. J., K. McAdam, M. M. Kaplan, J. D. Sipe, S. N. Vogel, and D. L. Rosenstreich. 1980. Monokine-induced synthesis of serum amyloid A protein by hepatocytes. *Nature.* **285:** 498–500.

5. Sipe, J. D., S. N. Vogel, J. L. Ryan, K. P. McAdam, and D. L. Rosenstreich. 1979. Detection of a mediator derived from endotoxin-stimulated macrohpages that induces the acute phase serum amyloid A response in mice. *J. Exp. Med.* **150:** 597–606.

6. Ridker, P. M., C. H. Hennekens, J. E. Buring, and N. Rifai. 2000. C-reactive protein and other markers of inflammation in the prediction of cardiovascular disease in women. *N. Engl. J. Med.* **342:** 836–843.

7. Badolato, R., J. M. Wang, W. J. Murphy, A. R. Lloyd, D. F. Michiel, L. L. Bausserman, D. J. Kelvin, and J. J. Oppenheim. 1994. Serum amyloid A is a chemoattractant: induction of migration, adhesion, and tissue infiltration of monocytes and polymorphonuclear leukocytes. *J. Exp. Med.* **180:** 203–209.

8. Furlaneto, C. J., and A. Campa. 2000. A novel function of serum amyloid A: a potent stimulus for the release of tumor necrosis factor-alpha, interleukin-1beta, and interleukin-8 by human blood neutrophil. *Biochem. Biophys. Res. Commun.* **268:** 405–408.

9. Lee, H. Y., M. K. Kim, K. S. Park, Y. H. Bae, J. Yun, J. I. Park, J. Y. Kwak, and Y. S. Bae. 2005. Serum amyloid A stimulates matrix-metalloproteinase-9 upregulation via formyl peptide receptor like-1-mediated signaling in human monocytic cells. *Biochem. Biophys. Res. Commun.* **330:** 989–998.

10. Song, C., K. Hsu, E. Yamen, W. Yan, J. Fock, P. K. Witting, C. L. Geczy, and S. B. Freedman. 2009. Serum amyloid A induction of cytokines in monocytes/macrophages and lymphocytes. *Atherosclerosis.* **207:** 374–383.

11. Wilson, P. G., J. C. Thompson, N. R. Webb, F. C. de Beer, V. L. King, and L. R. Tannock. 2008. Serum amyloid A, but not C-reactive protein, stimulates vascular proteoglycan synthesis in a pro-atherogenic manner. *Am. J. Pathol.* **173:** 1902–1910.

12. Christenson, K., L. Bjorkman, S. Ahlin, M. Olsson, K. Sjoholm, A. Karlsson, and J. Bylund. 2013. Endogenous acute phase serum amyloid A lacks pro-inflammatory activity, contrasting the two recombinant variants that activate human neutrophils through different receptors. *Front. Immunol.* **4:** 92.

13. Kim, M. H., M. C. de Beer, J. M. Wroblewski, N. R. Webb, and F. C. de Beer. 2013. SAA does not induce cytokine production in physiological conditions. *Cytokine.* **61:** 506–512.

14. de Beer, M. C., N. R. Webb, J. M. Wroblewski, V. P. Noffsinger, D. L. Rateri, A. Ji, D. R. van der Westhuyzen, and F. C. de Beer. 2010. Impact of serum amyloid A on high density lipoprotein composition and levels. *J. Lipid Res.* **51:** 3117–3125.

15. Jahangiri, A., M. C. de Beer, V. Noffsinger, L. R. Tannock, C. Ramaiah, N. R. Webb, D. R. van der Westhuyzen, and F. C. de Beer. 2009. HDL remodeling during the acute phase response. *Arterioscler. Thromb. Vasc. Biol.* **29:** 261–267.

16. van der Westhuyzen, D. R., L. Cai, M. C. de Beer, and F. C. de Beer. 2005. Serum amyloid A promotes cholesterol efflux mediated by scavenger receptor B-I. *J. Biol. Chem.* **280:** 35890–35895.

17. Annema, W., N. Nijstad, M. Tolle, J. F. de Boer, R. V. Buijs, P. Heeringa, M. van der Giet, and U. J. Tietge. 2010. Myeloperoxidase and serum amyloid A contribute to impaired in vivo reverse cholesterol transport during the acute phase response but not group IIA secretory phospholipase A(2). *J. Lipid Res.* **51:** 743–754.

18. Malik, P., S. Z. Berisha, J. Santore, C. Agatisa-Boyle, G. Brubaker, and J. D. Smith. 2011. Zymosan-mediated inflammation impairs in vivo reverse cholesterol transport. *J. Lipid Res.* **52:** 951–957.

19. McGillicuddy, F. C., M. de la Llera Moya, C. C. Hinkle, M. R. Joshi, E. H. Chiquoine, J. T. Billheimer, G. H. Rothblat, and M. P. Reilly. 2009. Inflammation impairs reverse cholesterol transport in vivo. *Circulation.* **119:** 1135–1145.

20. de Beer, M. C., J. M. Wroblewski, V. P. Noffsinger, A. Ji, J. M. Meyer, D. R. van der Westhuyzen, F. C. de Beer, and N. R. Webb. 2013. The impairment of macrophage-to-feces reverse cholesterol transport during inflammation does not depend on serum amyloid A. *J. Lipids.* **2013:** 283486.

21. De Beer, M. C., J. M. Wroblewski, V. P. Noffsinger, D. L. Rateri, D. A. Howatt, A. Balakrishnan, A. Ji, P. Shridas, J. C. Thompson, D. R. van der Westhuyzen, et al. 2014. Deficiency of endogenous acute phase serum amyloid A does not affect atherosclerotic lesions in apolipoprotein E-deficient mice. *Arterioscler. Thromb. Vasc. Biol.* **34:** 255–261.

22. Webb, N. R., M. C. De Beer, J. M. Wroblewski, A. Ji, W. Bailey, P. Shridas, R. J. Charnigo, V. P. Noffsinger, J. Witta, D. A. Howatt, et al. 2015. Deficiency of endogenous acute-phase serum amyloid A protects apoE-/- mice from angiotensin II-induced abdominal aortic aneurysm formation. *Arterioscler. Thromb. Vasc. Biol.* **35:** 1156–1165.

23. Sellar, G., S. Jordan, W. Bickmore, J. Fantes, V. Van Heyningen, and A. Whitehead. 1994. The human serum amyloid A protein (SAA) superfamily gene cluster: mapping to chromosome 11p15.1 by physical and genetic linkage analysis. *Genomics.* **19:** 221–227.

24. Kluve-Beckerman, B., M. L. Drumm, and M. D. Benson. 1991. Nonexpression of the human serum amyloid A three (SAA3) gene. *DNA Cell Biol.* **10:** 651–661.

25. Husebekk, A., B. Skogen, G. Husby, and G. Marhaug. 1985. Transformation of amyloid precursor SAA to protein AA and incorporation in amyloid fibrils in vivo. *Scand. J. Immunol.* **21:** 283–287.

26. Westermark, G. T., K. Sletten, A. Grubb, and P. Westermark. 1990. AA-amyloidosis. Tissue component-specific association of various protein AA subspecies and evidence of a fourth SAA gene product. *Am. J. Pathol.* **137:** 377–383.

27. Hoffman, J. S., L. H. Ericsson, N. Eriksen, K. A. Walsh, and E. P. Benditt. 1984. Murine tissue amyloid protein AA. NH2-terminal sequence identity with only one of two serum amyloid protein (ApoSAA) gene products. *J. Exp. Med.* **159:** 641–646.

28. Liepnieks, J. J., B. Kluve-Beckerman, and M. D. Benson. 1995. Characterization of amyloid A protein in human secondary amyloidosis: the predominant deposition of serum amyloid A1. *Biochim. Biophys. Acta.* **1270:** 81–86.

29. Kisilevsky, R., and S. P. Tam. 2003. Macrophage cholesterol efflux and the active domains of serum amyloid A 2.1. *J. Lipid Res.* **44:** 2257–2269.

30. Hoffman, J. S., and E. P. Benditt. 1983. Plasma clearance kinetics of the amyloid-related high density Lipoprotein apoprotein, serum amyloid protein (ApoSAA), in the mouse. *J. Clin. Invest.* **71:** 926–934.

31. Kluve-Beckerman, B., T. Yamada, J. Hardwick, J. J. Liepnieks, and M. D. Benson. 1997. Differential plasma clearance of murine acute-phase serum amyloid A proteins SAA1 and SAA2. *Biochem. J.* **322:** 663–669.

32. Parks, J. S., and L. L. Rudel. 1983. Metabolism of the serum amyloid A proteins (SSA) in high-density lipoproteins and chylomicrons of nonhuman primates (vervet monkey). *Am. J. Pathol.* **112:** 243–249.

33. Bausserman, L. L., P. N. Herbert, R. Rodger, and R. J. Nicolosi. 1984. Rapid clearance of serum amyloid A from high-density lipoproteins. *Biochim. Biophys. Acta.* **792:** 186–191.

34. Lowry, O. H., N. J. Rosebrough, A. L. Farr, and R. J. Randall. 1951. Protein measurement with the Folin phenol reagent. *J. Biol. Chem.* **193:** 265–275.

35. Bilheimer, D. W., S. Eisenberg, and R. I. Levy. 1972. The metabolism of very low density lipoprotein proteins. I. Preliminary in vitro and in vivo observations. *Biochim. Biophys. Acta.* **260:** 212–221.

36. de Beer, M. C., F. C. de Beer, W. D. McCubbin, C. M. Kay, and M. S. Kindy. 1993. Structural prerequisites for serum amyloid A fibril formation. *J. Biol. Chem.* **268:** 20606–20612.

37. Kieft, K. A., T. M. Bocan, and B. R. Krause. 1991. Rapid on-line determination of cholesterol distribution among plasma lipoproteins after high-performance gel filtration chromatography. *J. Lipid Res.* **32:** 859–866.

38. de Beer, M. C., A. Ji, A. Jahangiri, A. M. Vaughan, F. C. de Beer, D. R. van der Westhuyzen, and N. R. Webb. 2011. ATP binding cassette G1-dependent cholesterol efflux during inflammation. *J. Lipid Res.* **52:** 345–353.

39. Le, N. A., R. Ramakrishnan, R. B. Dell, H. N. Ginsberg, and W. V. Brown. 1986. Kinetic analysis using specific radioactivity data. *Methods Enzymol.* **129:** 384–395.

40. Cabana, V. G., J. N. Siegel, and S. M. Sabesin. 1989. Effects of the acute phase response on the concentration and density distribution of plasma lipids and apolipoproteins. *J. Lipid Res.* **30:** 39–49.

41. Feingold, K. R., I. Hardardottir, R. Memon, E. J. Krul, A. H. Moser, J. M. Taylor, and C. Grunfeld. 1993. Effect of endotoxin on cholesterol biosynthesis and distribution in serum lipoproteins in Syrian hamsters. *J. Lipid Res.* **34:** 2147–2158.

42. Grunfeld, C., M. Pang, W. Doerrler, J. K. Shigenaga, P. Jensen, and K. R. Feingold. 1992. Lipids, lipoproteins, triglyceride clearance, and cytokines in human immunodeficiency virus infection and the acquired immunodeficiency syndrome. *J. Clin. Endocrinol. Metab.* **74:** 1045–1052.

43. Sammalkorpi, K., V. Valtonen, Y. Kerttula, E. Nikkila, and M. R. Taskinen. 1988. Changes in serum lipoprotein pattern induced by acute infections. *Metabolism.* **37:** 859–865.

44. Cabana, V. G., J. R. Lukens, K. S. Rice, T. J. Hawkins, and G. S. Getz. 1996. HDL content and composition in acute phase response in three species: triglyceride enrichment of HDL a factor in its decrease. *J. Lipid Res.* **37:** 2662–2674.

45. Khovidhunkit, W., M. S. Kim, R. A. Memon, J. K. Shigenaga, A. H. Moser, K. R. Feingold, and C. Grunfeld. 2004. Effects of infection and inflammation on lipid and lipoprotein metabolism: mechanisms and consequences to the host. *J. Lipid Res.* **45:** 1169–1196.

46. Vaughan, A. M., and J. F. Oram. 2005. ABCG1 redistributes cell cholesterol to domains removable by high density lipoprotein but not by lipid-depleted apolipoproteins. *J. Biol. Chem.* **280:** 30150–30157.

47. Vaughan, A. M., and J. F. Oram. 2006. ABCA1 and ABCG1 or ABCG4 act sequentially to remove cellular cholesterol and generate cholesterol-rich HDL. *J. Lipid Res.* **47:** 2433–2443.

48. Acton, S., A. Rigotti, K. T. Landschulz, S. Xu, H. H. Hobbs, and M. Krieger. 1996. Identification of scavenger receptor SR-BI as a high density lipoprotein receptor. *Science.* **271:** 518–520.

49. Cai, L., M. C. de Beer, F. C. de Beer, and D. R. van der Westhuyzen. 2005. Serum amyloid A is a ligand for scavenger receptor class B type I and inhibits high density lipoprotein binding and selective lipid uptake. *J. Biol. Chem.* **280:** 2954–2961.

50. El Bouhassani, M., S. Gilibert, M. Moreau, F. Saint-Charles, M. Treguier, F. Poti, M. J. Chapman, W. Le Goff, P. Lesnik, and T. Huby. 2011. Cholesteryl ester transfer protein expression partially attenuates the adverse effects of SR-BI receptor deficiency on cholesterol metabolism and atherosclerosis. *J. Biol. Chem.* **286:** 17227–17238.

51. Cai, L., A. Ji, F. C. de Beer, L. R. Tannock, and D. R. van der Westhuyzen. 2008. SR-BI protects against endotoxemia in mice through its roles in glucocorticoid production and hepatic clearance. *J. Clin. Invest.* **118:** 364–375.

52. Rigotti, A., B. L. Trigatti, M. Penman, H. Rayburn, J. Herz, and M. Krieger. 1997. A targeted mutation in the murine gene encoding the high density lipoprotein (HDL) receptor scavenger receptor class B type I reveals its key role in HDL metabolism. *Proc. Natl. Acad. Sci. USA.* **94:** 12610–12615.

53. Hardardóttir, I., C. Grunfeld, and K. R. Feingold. 1995. Effects of endotoxin on lipid metabolism. *Biochem. Soc. Trans.* **23:** 1013–1018.

54. Khovidhunkit, W., R. A. Memon, K. R. Feingold, and C. Grunfeld. 2000. Infection and inflammation-induced proatherogenic changes of lipoproteins. *J. Infect. Dis.* **181(Suppl 3):** S462–S472.

55. Turnell, W., R. Sarra, I. D. Glover, J. O. Baum, D. Caspi, M. L. Baltz, and M. B. Pepys. 1986. Secondary structure prediction of human SAA1. Presumptive identification of calcium and lipid binding sites. *Mol. Biol. Med.* **3:** 387–407.

56. Booth, D. R., S. E. Booth, J. D. Gillmore, P. N. Hawkins, and M. B. Pepys. 1998. SAA1 alleles as risk factors in reactive systemic AA amyloidosis. *Amyloid.* **5:** 262–265.

57. Tam, S. P., A. Flexman, J. Hulme, and R. Kisilevsky. 2002. Promoting export of macrophage cholesterol: the physiological role of a major acute-phase protein, serum amyloid A 2.1. *J. Lipid Res.* **43:** 1410–1420.

58. Tape, C., and R. Kisilevsky. 1990. Apolipoprotein A-I and apolipoprotein SAA half-lives during acute inflammation and amyloidogenesis. *Biochim. Biophys. Acta.* **1043:** 295–300.

59. Jayaraman, S., C. Haupt, and O. Gursky. 2015. Thermal transitions in serum amyloid A in solution and on the lipid: implications for structure and stability of acute-phase HDL. *J. Lipid Res.* **56:** 1531–1542.

60. Meek, R. L., and E. P. Benditt. 1986. Amyloid A gene family expression in different mouse tissues. *J. Exp. Med.* **164:** 2006–2017.

61. Baranova, I. N., T. G. Vishnyakova, A. V. Bocharov, R. Kurlander, Z. Chen, M. L. Kimelman, A. T. Remaley, G. Csako, F. Thomas, T. L. Eggerman, et al. 2005. Serum amyloid A binding to CLA-1 (CD36 and LIMPII analogous-1) mediates serum amyloid A protein-induced activation of ERK1/2 and p38 mitogen-activated protein kinases. *J. Biol. Chem.* **280:** 8031–8040.

62. Lee, J. Y., J. M. Timmins, A. Mulya, T. L. Smith, Y. Zhu, E. M. Rubin, J. W. Chisholm, P. L. Colvin, and J. S. Parks. 2005. HDLs in apoA-I transgenic Abca1 knockout mice are remodeled normally in plasma but are hypercatabolized by the kidney. *J. Lipid Res.* **46:** 2233–2245.

63. Hammad, S. M., S. Stefansson, W. O. Twal, C. J. Drake, P. Fleming, A. Remaleyl, H. B. Brewer, and W. S. Argraves. 1999. Cubilin, the endocytic receptor for intrinsic factor-vitamin B12 complex, mediates high-density lipoprotein holoparticle endocytosis. *Proc. Natl. Acad. Sci. USA.* **96:** 10158–10163.

64. Hammad, S. M., J. L. Barth, C. Knaak, and W. S. Argraves. 2000. Megalin acts in concert with cubilin to mediate endocytosis of high density lipoproteins. *J. Biol. Chem.* **275:** 12003–12008.

65. Kozyraki, R., J. Fyfe, M. Kristianse, C. Gerdes, C. Jacobsen, S. Cui, E. Christensen, M. Aminoff, A. De La Chapelle, K. Krahe, et al. 1999. The intrinsic factor-vitamin B12 receptor, cubilin, is a high-affinity apolipoprotein A-I receptor facilitating endocytosis of high-density lipoprotein. *Nat. Med.* **5:** 656–661.

66. Ji, A., J. M. Wroblewski, L. Cai, M. C. de Beer, N. R. Webb, and D. R. van der Westhuyzen. 2012. Nascent HDL formation in hepatocytes and role of ABCA1, ABCG1, and SR-BI. *J. Lipid Res.* **53:** 446–455.

67. Wroblewski, J. M., A. Jahangiri, A. Ji, F. C. de Beer, D. R. van der Westhuyzen, and N. R. Webb. 2011. Nascent HDL formation by hepatocytes is reduced by the concerted action of serum amyloid A and endothelial lipase. *J. Lipid Res.* **52:** 2255–2261.

68. Julve, J., J. C. Escola-Gil, N. Rotllan, C. Fievet, E. Vallez, C. de la Torre, V. Ribas, J. H. Sloan, and F. Blanco-Vaca. 2010. Human apolipoprotein A-II determines plasma triglycerides by regulating lipoprotein lipase activity and high-density lipoprotein proteome. *Arterioscler. Thromb. Vasc. Biol.* **30:** 232–238.

69. Parks, J. S., and L. Rudel. 1985. Alteration of high density lipoprotein subfraction distribution with induction of serum amyloid A protein (SAA) in the nonhuman primate. *J. Lipid Res.* **26:** 82–91.

70. O'Brien, K. D., T. O. McDonald, V. Kunjathoor, K. Eng, E. A. Knopp, K. Lewis, R. Lopez, E. A. Kirk, A. Chait, T. N. Wight, et al. 2005. Serum amyloid A and lipoprotein retention in murine models of atherosclerosis. *Arterioscler. Thromb. Vasc. Biol.* **25:** 785–790.